The transition from density-driven to wave-dominated isolated flows.

RICHARD MANASSEH*
School of Mathematics, Fluid Dynamics Group,
University of New South Wales,
Sydney, NSW 2052, Australia

CHANG-YUN CHING & HARINDRA J. S. FERNANDO
Environmental Fluid Dynamics Program,
Department of Mechanical and Aerospace Engineering,
Arizona State University, Tempe, Arizona 85287, USA

* Current Affiliation:
Advanced Fluid Dynamics Laboratory, CSIRO DBCE,
PO Box 56, Highett, VIC 3190, Melbourne, Australia

Abstract

An isolated fluid mass travelling horizontally in a stratified layer is a phenomenon described alternatively as a detached gravity-current head or a strongly nonlinear solitary wave. A key feature of this flow is the transport of mass. Laboratory experiments examine the transition in time from a regime in which the flow is density driven, to one in which it is wave dominated. A simple means of creating this transitional regime, an isolated flow that exhibits both density and wave effects, is achieved by dropping a thermal into a linearly stratified layer. This transitional regime is called an 'isolated propagating

flow'. Parameters for which the transitional regime occurs are identified. Particle-tracking studies reveal the vertical flow structure. There is an upper zone that is wave-dynamical, and a lower zone in which transport of mass occurs. The transported mass slowly leaks out, until the phenomenon resembles a weakly nonlinear solitary wave. The experiments mimic a thunderstorm microburst impacting a temperature inversion, which has aviation safety implications. In the ocean, cracks in the ice cap (polar leads) cause similar flows impacting the thermocline.

1 Introduction

Gravity currents are density-driven phenomena that transport mass as a first-order effect. Solitary waves, like other fluid waves, transport momentum and energy. They travel unchanged in shape and form owing to a balance between nonlinearity and wave dispersion. However, weakly nonlinear solitary waves do not transport mass over long distances.

This paper is a study of an *isolated propagating flow*. Such disturbances are a transitional regime between a density-driven current propagating in a stratified layer and a weakly nonlinear solitary wave. They occur as initially density-driven flow evolves with time into wave-dominated flow. They create strong, oscillatory flow patterns in a medium that supports waves. They transport mass like a density-driven current, violating some precepts of wave mechanics. However, unlike the current, there is no upstream source of dense fluid driving the flow. Hitherto, such phenomena have been described either as detached gravity-current heads or as solitary waves. It could be argued that they are intensely nonlinear solitary waves. However, for the purposes of this paper a special terminology has been adopted to stress that neither description is wholly adequate. We base our definitions on the degree to which mass is transported. Thus *wave-dominated* behaviour is defined as a regime where mass transport has ceased. This is provided, of course, that other characteristics of wave-like behaviour (such as propagating oscillatory velocity and pressure fields) are present.

1.1 Gravity currents in stratified fluids

Much of the substantial body of research on gravity (or density) currents and related phenomena is summarized in the book by Simpson (1987). A gravity current is inherently a strongly nonlinear phenomenon that transports mass; unlike a solitary wave, it cannot be described using a weakly nonlinear correction to a linear solution. It has a well-known structure consisting of a raised head and a following flow. Within the head, near the bottom surface there is a feeder current that moves faster than the gravity-current propagation speed, and brings fluid to the top of the head. Thus there is a flow of transported mass through the head.

Gravity currents have been described by hydraulic theory (Benjamin 1968). A special case of a gravity current is relevant to the present paper; it is a gravity current propagating into a stably stratified layer. When a region of mixed fluid collapses into a stratified layer, a gravity current is formed if the height of the mixed-fluid region is considerably larger than the layer depth (Britter and Simpson 1981). If the mixed-fluid region is not so large, solitary waves may form (Maxworthy 1980). Under some circumstances, the head of the gravity current may detach from the following flow and travel ahead as an isolated 'blob' of fluid (Maxworthy 1980), having a similar appearance to a solitary wave. The leading portion of the following flow may then develop a new head which can subsequently detach as well (Simpson 1987). Whenever a head 'detaches', however, there is always a thin trail of dense fluid leaking out behind it. Numerical calculations by Hasse and Smith (1989) showed that a gravity current propagating into a stable layer could spawn from its head a solitary-wave-like disturbance with closed circulation.

1.2 Solitary waves in stratified fluids

Considerable research has been done on solitary waves in stratified fluids. Long (1953) presented an integral of the momentum equation along a streamline in a form appropriate to stratified fluids, which has been used in much subsequent analysis. Solitary waves in deep fluids containing a thin stratified layer were first treated analytically by Benjamin (1967) and independently by Davis & Acrivos (1967) and Ono (1975). An equation, usually called the Benjamin-Davis-Ono (BDO) equation after its discoverers, can be derived for a system in which weak nonlinearity balances wave dispersion. The BDO equation is for the horizontal wave structure and admits soliton solutions. The BDO equation is appropriate to an upper boundary condition of an infinite, neutrally stratified layer overlying the pycnocline. If a 'rigid lid' tops the pycnocline, the Korteweg–de Vries (KdV) equation is the appropriate formulation.

Numerical work reported by Davis & Acrivos (1967) was based on Long's equation, as was more recent numerical work by Tung et al (1982), extended by Brown & Christie (1994). These calculations show a topological change in the vertical structure once the amplitude becomes large relative to the thickness of the stratified layer. A recirculation zone or region of closed streamline flow forms, which must contain mass transported with the wave. This invalidates the principle of a continuous streamline with known upstream conditions, on which Long's equation and the calculations are based.

Davis & Acrivos (1967) also showed experimentally that 'lumps' of fluid appeared to travel with the wave propagation velocity and regions of closed streamline flow were often observed. Since then, several authors (notably Stamp & Jacka 1995) have observed similar phenomena, where mass appears to be transported with the solitary wave. Stamp & Jacka (1995) studied solitons on a thin density interface. They observed counter-rotating cells which were not true closed-streamline regions, with fluid continually being entrained into and ejected from the cells. No other investigations of the vertical structure within the wave have been reported, though in experiments referred to above, transported mass was reported to appear turbulent.

The observed speeds of solitary waves have generally agreed with numerical solutions to Long's equation. However, the vertical structure of the wave, incorporating the mass-transporting recirculation zone, is hard to predict. This vertical structure is likely to be of great practical importance to flows in the environment.

1.3 Environmental evidence for a transitional regime

There are atmospheric and oceanic applications where wavelike disturbances transporting mass play an important role. There may also be geological situations within the earth where these phenomena are important; solitary disturbances transporting mass are thought to be relevant to physics in the earth's mantle (Grimshaw et al 1992). In the ocean, polar 'leads' are thin, long cracks caused by plastic failure of the ice cap. In the winter, the exposed water re-freezes immediately, generating plumes and thermals of increased-salinity water. These may generate disturbances transporting mass on impacting a thermocline below (Noh et al 1992).

Among the atmospheric phenomena is the gust front created in a stratified atmosphere (a low-level temperature inversion) by a thunderstorm outflow. Relevant observations and analyses include those of Shreffler & Binkowski (1981), Fulton et al (1990), Doviak & Ge (1984), Doviak et al (1991) and Manasseh & Middleton (1995). These disturbances are thought to be a hazard to aircraft because they transport unpredictable wind shear far from the original thunderstorm outflow (Doviak & Christie 1989). A pilot negotiating the disturbance should understand its vertical structure in particular.

Comparisons with weakly-nonlinear wave theory work best for large-scale atmospheric disturbances, not thunderstorm phenomena. An example is the mesoscale 'Morning Glory' of northern Australia (Clarke et al 1981; Haase & Smith 1984; Christie 1992; Alpers & Stilke 1996). However, even in these cases, a wave amplitude must often be chosen that probably renders the weak nonlinear assumption invalid. This makes successful results possibly fortuitous (Rottman & Einaudi 1993).

In general, weakly-nonlinear wave theory has been used with some success, albeit with decreasing mathematical validity, for amplitudes up to about half the stratified layer thickness. Usually the wave speed can be well matched by weakly nonlinear theory, but the structure is poorly predicted (Noonan & Smith 1985, Manasseh & Middleton 1995). Supporting these observational findings, the experiments of Stamp & Jacka (1995) found the wavelength-amplitude relationship predicted by weakly nonlinear theory broke down at larger amplitudes. Analytic and numerical work that permits full nonlinearity, subject to a constant-vorticity assumption, shows that the streamline structure alters greatly as amplitude increases (Pullin & Grimshaw 1988; Forbes & Belward 1996; Evans & Ford 1996).

Laboratory realizations of the scenario in which gravity currents engender solitary waves are given by the experiments of Rottman & Simpson (1989). Laboratory thermals hitting a density interface – a situation which models ploar leads and perhaps also thunderstorm events – were shown to generate solitary waves by Noh et al (1992).

To summarize §1.1 - §1.3, there exist conceptual and analytical tools based on hydraulics used to treat density-driven currents (e.g. Benjamin 1968), and tools based on wave mechanics that are useful for describing solitary waves (e.g. Benjamin 1967). These models have separate theoretical bases that do not overlap. However, it appears that nature can produce a hybrid: an isolated propagating flow, which appears during the transition in time from density-driven to wave-dominated flow.

In the present experiments, the use of a thermal to create the disturbance is thought to be a natural way of generating an isolated propagating flow. The thermals and isolated propagating flows were chosen to be two-dimensional. The isolated propagating flows are to be created in a linearly stratified layer immediately overlying a solid boundary. This has the advantage of being a system for which an analytical solution under linear and weakly nonlinear theory is available.

The experiments are also an analogue of a linear thunderstorm microburst impacting a temperature inversion overlying the ground. (Many microbursts are axisymmetric in form, and hence evolve differently to the ones studied here. However, linear microbursts also occur, formed by several axisymmetric microbursts along a line. These are thought to pose a greater aviation hazard than individual axisymmetric microbursts (Hjelmfelt 1988).)

The paper is organized as follows. §2 explains the experiment. Section 3.1 outlines an appropriate weakly nonlinear theory for solitary waves, §3.2 describes methods of summarizing the results non-dimensionally. §4 describes the results and in §5 some discussion of the significance of the results is presented.

2 Experimental system and method

A Perspex tank of dimensions 243 x 31 x 61 cm was used; see figure 1 for a schematic view. The tank was filled with a homogeneous fluid layer on top of a linearly salt-stratified layer. The stratified layer was made by the two-tank method of Oster & Yamamoto (1963). First, the

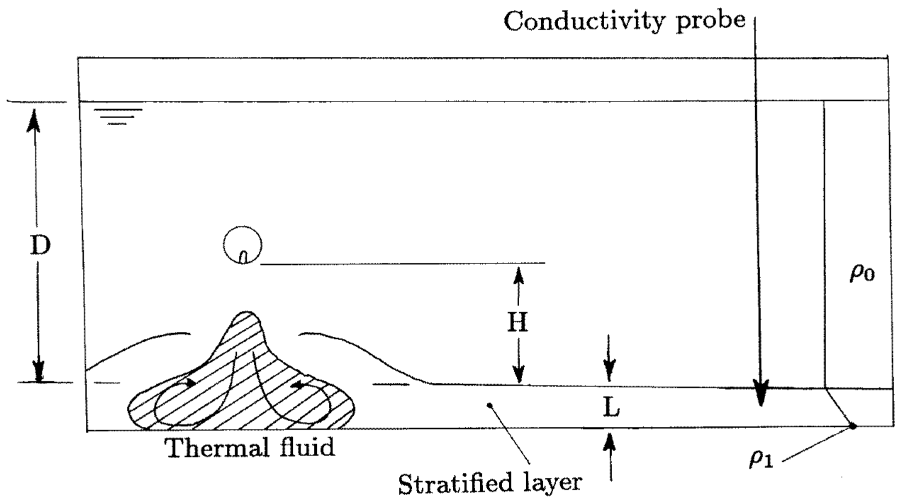

Figure 1: Schematic diagram of the experimental apparatus.

homogeneous layer of density ρ_0 was added to the desired depth D and then the stratified layer was fed underneath, via a capped hole located at the bottom of the tank, to a depth L. After filling the tank it was left to stand for 1 hour. Care was taken to prevent a steep density jump between the homogeneous layer and the stratified layer by preparing a single stock of water for the homogeneous layer and the less-dense tank of the two-tank filling system. The tank filling was checked using the density profile obtained with a traversing conductivity probe. The stratification was repeatable within ± 0.4 kg m^{-3} of the target salinity at the bottom of tank filling.

The thermal was salt water of a density greater than the maximum stratified layer density. A cylindrical tube with a thin slot spanning the tank contained the desired thermal volume. It was pivoted on the tank walls. To generate the thermal the tube was rapidly inverted. Just prior to releasing the thermal, potassium permanganate crystals were placed on the tank floor about 5 cm to the right of the thermal impact point. The thermal on striking the bottom and on entraining

Experiment Number	H cm		ρ_1 kg m^{-3}		ρ_t kg m^{-3}		V_0 ml	
1.131	5.0	± 0.2	1004.1	± 0.4	1073.9	± 0.4	22	± 1
1.240	5.0	± 0.2	1008.9	± 0.4	1120.0	± 1.0	22	± 1
1.330	10.0	± 0.2	1002.7	± 0.4	1107.5	± 0.3	22	± 1
4.150	3.5	± 0.2	1003.4	± 0.3	1160.0	± 0.3	22	± 1
Minimum	2.0	± 0.2	1002.5	± 0.5	1020.0	± 1.0	30	± 1
Maximum	10.0	± 0.2	1012.1	± 0.4	1200.0	± 1.0	9	± 1

Table 1: Typical initial parameters for some experiments, together with maximum and minimum values tried for each parameter. H is defined in figure 1; ρ_1 : density of the bottom of the stratified layer (the homogeneous layer had density 1000 kg m^{-3} for dye experiments); ρ_t : density of the thermal. Variations in error bounds were caused by unavoidable variations to experiment preparation methods.

the potassium permanganate became purple in colour. This served to identify the thermal fluid.

In some experiments the flow was visualized by dying the fluid layers, which were viewed using a shadowgraph method. To differentiate the different layers, methylene blue was added to the homogeneous layer, and a thin layer of fluorescein dye was introduced between the homogeneous and stratified layers.

The linearity and buoyancy frequency of the stratified layer was checked and calculated from the density profile. Speeds of propagation of the thermal and subsequent phenomena were measured in situ with a stopwatch and checked against the video tape measurements. The amplitude of the phenomenon was measured from the video recordings. Conductivity measurements were also taken during the experiments at a depth of 1 cm above the bottom of the tank and 80 cm from the initial thermal position. The conductivity measurements were used only as a check, since by the time the phenomenon reaches the probe its amplitude is substantially reduced.

Experiments were also performed with the system seeded by neutrally-buoyant particles, in order to obtain data on the mass-transporting vertical structure by particle tracking. For these experiments, the density of the homogeneous layer was chosen to ensure that the particles (specific gravity $\sim$ 1.04 and diameter 1.08 - 1.46 mm) resided in the stratified layer. The DigImage software package was used to obtain data on the particle locations and tracking parameters. These were processed using independent software to create particle pathlines.

3 Theoretical notes

3.1 The wave-dynamics regime

Disturbances of wavelength λ propagating in a fluid layer of depth D and stratification depth L (see figure 1) can be classified into three categories (Stamp & Jacka 1995); shallow-water waves ($\lambda/D \gg 1$, $L/D = O(1)$), deep-water waves ($\lambda/D \to 0$, $\lambda/L \gg 1$) and finite-depth waves ($L/D \ll 1$, $\lambda/L \gg 1$). In atmospheric and oceanic flows of interest here, the wavelengths are much smaller than the total depth of fluid, but they are much longer than the thickness of the stratified layer. Hence the interest here is on deep-water waves.

The deep-water waves can be linear, weakly nonlinear or strongly nonlinear, depending on their normalized amplitude a/L. In the experiments reported here, the flows are mostly in the strongly nonlinear regime. Details of the linear and weakly nonlinear theories have been given elsewhere (Benjamin 1967, Davis & Acrivos 1967) and these theories were placed in an atmospheric context by Rottman & Einaudi (1993) and Manasseh & Middleton (1995).

The buoyancy frequency of the lower layer, $N^2(z)$, is given by

$$N^2(z) = -\frac{g}{L}\frac{1}{\rho}\frac{\mathrm{d}\rho}{\mathrm{d}z}, \tag{1}$$

where ρ is the hydrostatic density. For the experiments considered here, the stratification is linear, so N is a constant. This also means there is a straightforward solution to the linear and weakly nonlinear equations of motion. This gives the propagation speed of the disturbance, c, for boundary conditions of a thin stratified layer underlying a deep neutrally stratified layer (appropriate to the BDO equation) as

$$c = c_0 + \bar{a}c_1, \tag{2}$$

where $\bar{a}$ is the maximum vertical streamline displacement a, nondimensionalized by L, and the linear eigenvalue or wave speed is given by

$$c_0 = \frac{2NL}{(2n-1)\pi}, \quad n \in \{1, 2, 3...\}, \tag{3}$$

for the nth mode. If rigid-lid (KdV-equation) boundary conditions are used, c_0 is given by

$$c_0 = \frac{NL}{n\pi}. \tag{4}$$

Equation (2) is plotted in figure 6, which will be described in §4.1. It is expected that linear or weakly nonlinear theories would be of limited relevance here; as noted in §1.2, they cannot predict mass transport. However it is important to note the wave speeds linear or weakly nonlinear theories predict. Some recent fully nonlinear theories are those of Pullin & Grimshaw (1988), Forbes & Belward (1996) and Evans & Ford (1996), and numerical calculations include those of Tung et al (1982) and Brown & Christie (1994).

3.2 Dimensional analyses

For the system described in figure 1, the important governing parameters are Q_0, H, L, x, and N. Here, the total buoyancy of the thermal, Q_0, is given by $\delta b_0 V_0$ (Noh et al 1992), where V_0 is the initial volume of thermal fluid per unit length, and the initial buoyancy deficit is $\delta b_0 = g(\rho_t - \rho_0)/\rho_0$, ρ_t being the density of the thermal fluid and ρ_0 the density of the upper (homogeneous) layer. Given typical average measured speeds and lengthscales, the Reynolds number for the horizontal component of flow is about 2000. The Reynolds number decreased with the evolution of the flow; hence viscous bottom-frictional effects are expected to dominate the horizontal propagation only at large x. The depth D of the upper layer has not been considered a parameter in view of the assumption $L/D \ll 1$. It will be confirmed in §4.1 that D is not a factor in the system. Also note that Q_0 effectively has dimensions $\mathrm{L}^3\mathrm{T}^{-2}$ because two-dimensional flow is being considered.

For simplicity, consider the horizontal speed of propagation c of the disturbance, which should depend on Q_0, x, H, L and N. The analysis is restricted to averages over a specific region of x. Then c can be written as

$$c = c(H, L, N, Q_0). \tag{5}$$

Since there are five variables in (5), c when non-dimensionalized will depend on two non-dimensional parameters. They are N^2H^3/Q_0 and H/L, and their significance can be explained as follows.

Consider the density-driven fall of the thermal. The bulk of its motion, for $H \gg L$ as is the case here, occurs in homogeneous fluid. Thus its speed on impacting the stratified layer scales as $(Q_0/H)^{1/2}$ (Noh & Fernando 1992), and its length scale l_H is proportional to H. (The constant of proportionality is about 0.6). After impact the thermal mass must deflect horizontally, splitting into a pair of opposite-travelling vortices. Experiments on descending line thermals show that these vortices are initially driven by the change in momentum imparted by the impact. However, after travelling a distance of about $1.5 l_H$ the motion is once more density-driven. Both momentum and density-driven motions still scale with $(Q_0/H)^{1/2}$.

Since the length scale of the thermal on impact is $l_H \sim H$, the largest possible speed scale of any internal wave motions generated on impact is NH. The ratio of this to the density-driven speed scale $(Q_0/H)^{1/2}$ gives the parameter N^2H^3/Q_0. When N^2H^3/Q_0 is very small, even the largest wave motion is much smaller than density-driven effects. Meanwhile, the parameter H/L could represent the initial potential energy of the thermal, relative to that of the stratified layer disturbed by a mass with the same buoyancy deficit.

We will now non-dimensionalize c using physical reasoning, firstly assuming the flow has aspects of density-driven behaviour, and secondly assuming it is wave dominated.

For the density-driven regime and also the transitional regime, in which density-driven effects continue to play a role, the propagation speed c should scale with $(Q_0/H)^{1/2}$. Therefore an appropriate non-dimensionalization for both density-driven and transitional regimes is

$$\frac{c}{(Q_0/H)^{1/2}} = f_1\left(\frac{H}{L}, \frac{N^2H^3}{Q_0}\right), \tag{6}$$

where $f_1, f_2 \ldots$ are functions.

Eventually, the flow is expected to dominated by the wave mechanics of the stratified layer. Now, following (3) and (4), the propagation speed should scale with NL. An appropriate non-dimensionalization is

$$\frac{c}{NL} = f_2\left(\frac{H}{L}, \frac{N^2H^3}{Q_0}\right). \tag{7}$$

The scalings (6) and (7) will be used to interpret experimental results.

4 Results

4.1 General evolution of the phenomenon, speed and amplitude

Initial trials were undertaken to optimize the system. The intent was to maximize the physical amplitude of the phenomenon, in order to facilitate observations of its vertical structure, in particular, the mass-transporting part. This meant maximizing the stratified layer depth L; however, if L was too large, significant wave motion did not occur, because a given impact applied to the layer resulted in a smaller amplitude when scaled by L. Attempts to create larger impacts by releasing larger thermal volumes resulted in excessive mixing. The ratio L/D had to be minimized, where D is the depth of the upper layer; if L/D was too large, the system was tending to a regime governed by the 'rigid-lid' boundary condition (4), which is less desirable since it has limited relevance to the atmospheric application. The upper layer depth D was limited by practical considerations: if D was too large, the Perspex tank walls had substantial deflections at the mid levels, introducing optical distortion.

The optimal stratified layer depth L of 2 cm was used in all experiments. For consistency with the analysis in §3.1, L is used as a general length scale, and dimensionless distances quoted below are non-dimensionalized with L. The optimal value of D was 20 cm; however, as a check experiments were also run with $D = 40$ cm, as will be described shortly. Typical values of the parameters for some experiments are given in table 1, together with maximum and minimum ranges.

Schematic drawings of typical stages in the flow evolution are given in figure 2. By the time the thermal reaches the top of the stratified layer it has entrained sufficient fluid to have expanded to a diameter several times the stratified layer thickness. The height of the thermal vortices after impact depends on H/L; typically the thermal-vortex height is 3–4 times the layer depth for $H/L = 2.5$, for example. The thermal forms a roll vortex on either side of the impact centreline. Up to about $x = 5$–10 non-dimensional units (10–20 cm), its behaviour appears essentially as any of the several well-documented cases of a vortex pair or vortex ring impacting a solid boundary. Examples include the work of Linden & Simpson (1985), Lundgren et al (1992) and Orlandi & Verzicco (1993). The flow in the thermal vortex is turbulent, but the length scales of motions within the thermal appear small relative to the thermal vortex, about $1/5$ its size or less. This stage is shown in figure 3(a), in which the vortices are unclear but the typical scale of the thermal impact can be seen. It is also shown diagrammatically in figure 2(a).

For some combinations of parameters, chiefly for low Q_0 and strong N, the thermal vortex quickly collapses and forms a weak intrusion that only travels to $x = 20$ or so. No waves are visible on the stratified layer. Significant motions cease quickly.

For many regions of parameter space, however, the thermal mass travels to $x = 40$ or beyond, enclosed in a solitary 'hump' of stratified layer fluid, as illustrated in figures 2(c) and (d) and figures 3(c) and (d), where the thermal mass appears purple. The length of the 'hump' is typically about 5 times the layer depth. This phenomenon represents the transition from a density-driven to a wave-dominated flow. It will be called an 'isolated propagating flow' (IPF) and its evolution is as follows.

By the time the IPF reaches about $x = 10$–15, the thermal mass within it has flattened out and taken a more elliptical shape, still clearly rotating in the same sense as the original thermal vortex at the impact. The stratified-layer fluid, which had been thrown up above the thermal vortex, now covers the thermal mass. Dye distributions show that the stratified-layer fluid remains quite distinct from the

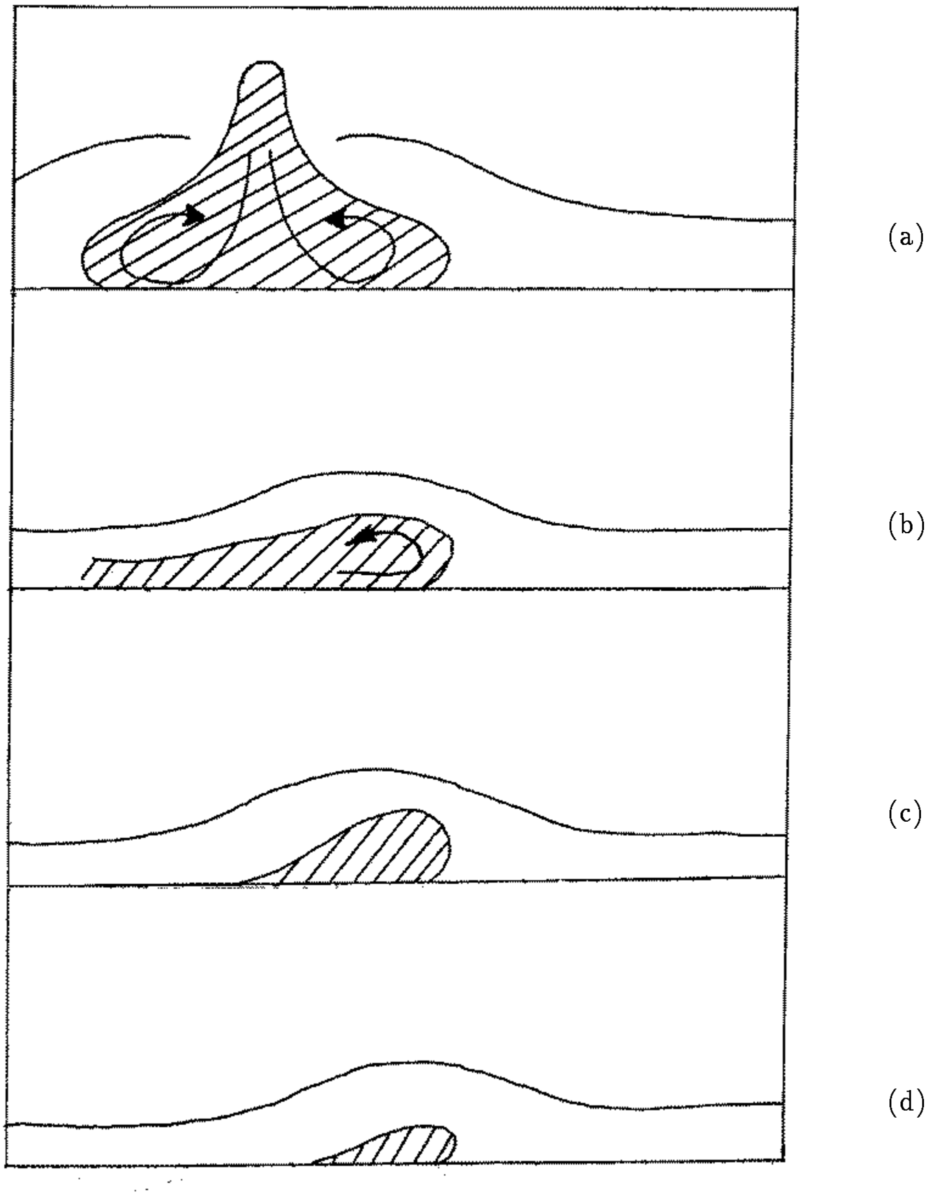

Figure 2: Typical stages in the flow evolution. See text for explanations.